PHYSICAL REVIEW C **82**, 011901(R) (2010)

Multistrange particle production and the statistical hadronization model

Michal Petráň[1,2] and Johann Rafelski[1]
[1]*Department of Physics, University of Arizona, Tucson, Arizona 85721*
[2]*Department of Physics, Czech Technical University, Brehova 7, 11519 Praha 1*
(Received 9 December 2009; revised manuscript received 17 May 2010; published 26 July 2010)

We consider the chemical freeze-out of Ξ, $\overline{\Xi}$, and ϕ multistrange hadrons within a statistical hadronization model inspired approach. We study particle yields across a wide range of reaction energy and centrality from NA49 at the Super Proton Synchrotron (SPS) and the Solenoidal Tracker at RHIC (STAR) experiments. We constrain the physical conditions present in the fireball source of strange hadrons and anticipate results expected at the Large Hadron Collider (LHC).

DOI: 10.1103/PhysRevC.82.011901 PACS number(s): 24.10.Pa, 12.38.Mh, 13.60.Rj, 25.75.−q

Introduction—We study multistrange hadron production in the context of the quark-gluon plasma (QGP) formation in relativistic heavy ion collisions [1]. Given the relatively small reaction cross sections of multistrange hadrons in hadron matter, the observed yields of $\Xi(qss)$, $\overline{\Xi}$, $\Omega(sss)$, $\overline{\Omega}$, $\phi(s\bar{s})$ [2–7] are considered probes of the earliest stage of the QGP-fireball hadronization.

The yields of these particles were considered previously within a global approach (see, e.g., Ref. [8]). Here we show that it is possible to analyze multistrange hadron yields alone. When this is done we find that multistrange and nonstrange hadrons share the same freeze-out condition. We will discuss the meaning of this discovery in the following, addressing the dynamics of hadronization. We also address the forthcoming Large Hadron Collider (LHC) effort to measure multistrange hadron yields in high multiplicity pp [9], and soon after, in A + A reactions.

QGP hadronic particle production yields are usually considered within the statistical hadronization model (SHM) [10–12]. SHM has been successful in describing (strange) hadron production in heavy ion collisions for different colliding systems and energies. These results showing successful global fits of particle yields in the SHM framework inspired us to study multistrange hadron yields alone in this separate analysis for the purpose of (i) establishing that SHM is appropriate for describing yields of these particles, (ii) assessing if their yields are consistent with the established bulk matter properties of the QGP fireball, thus testing the single freeze-out hypothesis for particles with large and small hadron reaction cross sections, and (iii) understanding better how the future LHC results may help arrive at a distinction between SHM model approaches.

SHM Models—We begin by introducing the three principal SHM approaches:

(i) Taking the view that SHM has a limited theoretical foundation, one can seek *simplicity* in an effort to obtain a qualitative description of the yields for all hadrons with just a small number of parameters. An additional attraction is that this assumption leads to a model with chemical equilibrium hadron yields is explored. The main result of this approach is that the hadronization in high-energy heavy ion collisions at the Relativistic Heavy Ion Collider (RHIC) requires $T \geqslant 175$ MeV and this high value is close to the lattice crossover temperature, between the deconfined and hadron phases [13,14].

(ii) To arrive at a precise description of the bulk properties, such as the strangeness and entropy content of the hadron fireball, we need a precise capability to extrapolate hadron yields to unobserved kinematic domains and particle types. This is achieved by introducing statistical occupancy parameters $\gamma_i > 1, i = q, s$. Within this approach there is good systematic behavior of physical observables as a function of collision conditions such as energy or centrality [8,15–19]. The yields of hadrons are, in general, found not to be in chemical equilibrium, $\gamma_i \neq 1$; the hadronization temperature is found near to $T \simeq 140$ MeV.

While this value of T can be further away from the deconfinement crossover domain, this is where chiral symmetry restoration is achieved [13,20] and QGP is transformed into hadrons. Moreover, in this approach the variation of the freeze-out temperature with a baryochemical potential parallels the slope seen in the lattice data. Another important outcome of this approach is that a fit to the data offers a good statistical significance. The results obtained can be interpreted in terms of a dynamical picture of nearly chemically equilibrated QGP, decaying into free streaming hadrons. The high intrinsic QGP entropy content explains why equilibrated QGP turns into chemically overpopulated (oversaturated) hadronic gas (HG) phase space—the fast breakup of QGP means that the emerging hadrons do not have the opportunity to re-establish chemical equilibrium in the HG phase.

(iii) The *single freeze-out* and/or *strangeness nonequilibrium* model has, as the main objective, a statistically significant description of hadron yields achieved with minimal effort. Only strangeness chemical nonequilibrium is allowed. This is often enough to produce a decent data fit and to assure that all particles can be formed at the same physical condition [21–25]. The main result of this approach is a hadronization temperature near $T \simeq 160$ MeV, which agrees with Hagedorn temperature [26,27].

Particle ratios of interest—We must include in our theoretical consideration of multistrange hadron yields the contributing yield of decaying hadron resonances. Within SHM these individual yields generally depend on several parameters. The phase-space occupancy γ_q scales particle yields according to the light quark content and a similar parameter γ_s refers to the strange quark content. Temperature T quantifies the size of the accessible phase space. The baryochemical potential μ_B differentiates baryons from antibaryons and strange chemical potential μ_S does the same for strangeness. There is also a potential μ_{I3} related to a different number of up and down quarks that is constrained by proton and neutron asymmetry in colliding nuclei and the overall yield is normalized by a volume parameter V.

By considering the ratio

$$\frac{\Xi}{\phi} \equiv \sqrt{\frac{\overline{\Xi}^+\Xi^-}{\phi\phi}} \simeq \gamma_q f(T), \tag{1}$$

we eliminate in good approximation most of the SHM parameter dependencies since (i) by taking the product of a particle and antiparticle, we eliminate baryochemical potential μ_B as well as strange chemical potential μ_S, (ii) we also eliminate the strange quark phase-space occupancy γ_s because the strange and antistrange quark content in the numerator and denominator is the same, and (iii) The overall normalization is eliminated by the fact that we have the same number of hadrons in the ratio numerator and denominator.

The Ξ/ϕ ratio depends on the probability of finding a nonstrange $d, \bar{d}$ quark at the formation of $\Xi^-(dss)$ and $\overline{\Xi}^+(\bar{d}\bar{s}\bar{s})$, respectively. This is expressed by the light quark phase-space occupancy γ_q. Furthermore, temperature T controls the magnitude of

$$f(T) \simeq \sum_i \frac{g_i}{3}\left(\frac{m_{\Xi_i}}{m_\phi}\right)^{3/2} e^{\frac{m_\phi - m_{\Xi_i}}{T}}, \tag{2}$$

the (nonrelativistic) phase-space ratio of Ξ^- and ϕ. $\Xi(1321)$ is always a decay product of $\Xi^*(1530)$. Thus aside from the ground state $i = 1 : \Xi(1321)$, $g_1 = 2$ one must include in the sum the $\Xi^*(1530)$, $g_2 = 4$ resonance. Consideration of this special yield ratio parallels the earlier effort made to identify γ_s/γ_q in Ref. [28].

We extend our considerations to include single strange $K^+(u\bar{s})$, $K^-(\bar{u}s)$ mesons and triple strange $\Omega^-(sss)$, $\overline{\Omega}^+(\bar{s}\bar{s}\bar{s})$ baryons considering the ratios

$$\frac{\Xi}{K} \equiv \sqrt{\frac{\overline{\Xi}^+\Xi^-}{K^+K^-}} = \gamma_s f_1(T); \quad \frac{\Omega}{\phi} = \sqrt{\frac{\overline{\Omega}^+\Omega^-}{\phi\phi}} = \gamma_s f_2(T). \tag{3}$$

Given the quark content, both Ξ/K and Ω/ϕ are proportional to strange quark yield [i.e., the strange quark phase-space occupancy γ_s and a function $f_i(T)$].

The arguments leading to Eq. (1) and Eq. (3) are strictly valid only in the Boltzmann approximation. Considering quantum statistics, there is some residual dependence of $f(T)$ on the chemical parameters, involving higher powers of γ_q for the ratio Ξ/ϕ Eq. (1), and higher powers of γ_s for the ratio Ξ/K Eq. (3). To estimate the magnitude of the quantum statistics effect we calculate the actual particle ratios with SHARE2 [11] using both quantum and Boltzmann statistics. We find that the Boltzmann approximation we used overestimates Ξ/ϕ by 0.25%, which is always negligible. For Ξ/K, we find that it is overestimated by the Boltzmann approximation by up to 4%, the relatively larger effect is due to the relatively low mass of the kaon. Since the experimental error is much greater we continue to consider the simple theoretical Boltzmann yields. When in the following we consider ratios involving pions, all results are obtained using SHARE2, which accounts for resonance decays and all yields can be obtained using quantum statistics.

Experimental data—We consider 4π data from the CERN-SPS NA49 experiment, and for the STAR experiment at RHIC the acceptance rapidity interval is $|y| < 0.5$; therefore at RHIC we use the yield per unit of rapidity dN/dy and omit the differential dy when referring to relative yields. For the ϕ meson we consider the recently published data from STAR [2] and the updated data from NA49 [3]. We collected the necessary data for Ξ and $\overline{\Xi}$ baryons from Refs. [4–6].

We do not use NA49 158 GeV results since these experimental results do not allow us to interpolate the different centrality bins used to measure different multistrange particle yields. We cannot simply combine data from different centrality bins having seen the variation of yields with centrality (that is γ_s). The STAR 62 experiment provides data in several centrality bins, defined as a percentage of the most central collisions: Data from the most central collisions are found in the centrality 0–5% interval and the most peripheral collision results presented are in the 70–80% bin. The relation to N_{part} and/or impact parameter b is discussed in Ref. [7].

We use recent data for $K^\pm$ mesons from STAR experiments at both $\sqrt{s_{NN}} = 200$ and 62.4 GeV from Ref. [7]. For the SPS NA49 data we use yields from Refs. [29,30].

We note that different centrality bins are often chosen for different particle types. To be able to form particle ratios in a common centrality interval, we interpolate or extrapolate, that is, fit individual yields as a function of the number of participants using a simple functional form $f(N_{\text{part}}) \equiv a \cdot N_{\text{part}}^b + c$. We show the fit parameters a, b, and c in Table I and compare the experimental results and the fit in Fig. 1.

TABLE I. Fit parameters used to determine particle yields for incompatible centrality bins using $f(N_{\text{part}}) \equiv a \cdot N_{\text{part}}^b + c$ (see text for details).

	a	b	c
π^-	4.179×10^{-1}	1.072	7.107×10^{-1}
π^+	4.247×10^{-1}	1.048	6.422×10^{-1}
K^+	5.433×10^{-2}	1.111	-1.014×10^{-1}
K^-	4.812×10^{-2}	1.107	-3.859×10^{-2}
Ξ^-	1.228×10^{-3}	1.247	-4.678×10^{-3}
$\overline{\Xi}^+$	8.978×10^{-4}	1.221	9.390×10^{-4}
ϕ^0	4.162×10^{-3}	1.203	-9.311×10^{-3}

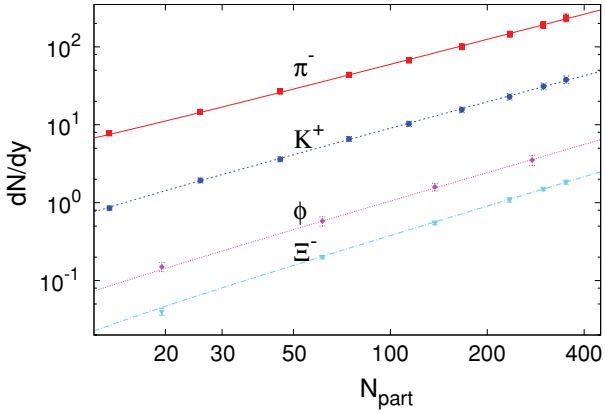

FIG. 1. (Color online) Data points (full symbols) of particle yields used in the analysis and their respective fitted centrality dependence.

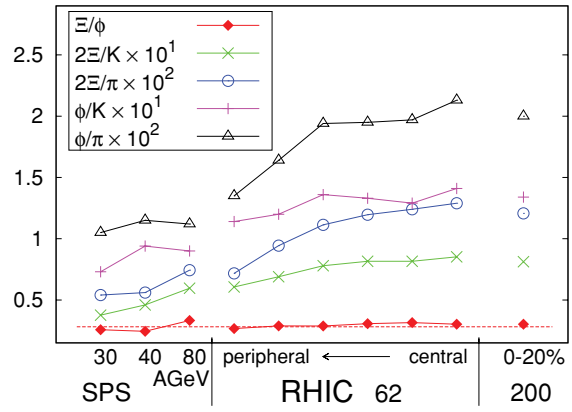

FIG. 2. (Color online) Data points of Ξ/ϕ Eq. (1), Ξ/K Eq. (3), Ξ/π and ϕ/π Eq. (4). The straight line for $\Xi/\phi = 0.281$.

Particle ratios—After this preparation we can form ratios of particle yields as shown in Fig. 2 and Table II. We note that the Ξ/ϕ relative yield does not change much over a wide range of energies and centralities, in contrast to the individual hadron yields which enter the ratio. The average value of all available data points is $\Xi/\phi = 0.281$ with an error at 15% level.

The remarkable result, the constancy of Ξ/ϕ, means that at SPS and RHIC energies the mechanisms and conditions at which double-strange particles are produced are very similar and that, according to Eq. (1), there is a constraint between the values of γ_q and T, which we now explore in Fig. 3 where we show in the T, γ_q plane the theoretical SHM results as lines for a constant ratio Ξ/ϕ. These values are obtained using SHARE2 and varying γ_q and T, with all other model parameters fixed to reasonable physical values. In this way we also confirm once again the analytical formula Eq. (2).

We limit the magnitude of γ_q by a critical value of light quark phase-space occupancy $\gamma_q^{\rm crit}$. $\gamma_{\pi^0} \equiv \gamma_q^2 \leqslant (\gamma_q^{\rm crit})^2 = \exp(m_{\pi^0}/T)$, which is the condition where the pion phase-space distribution function diverges for $m_{\pi^0} = 135$ MeV/c^2. The experimental values $\Xi/\phi \simeq 0.281 \pm 15\%$ are found consistent with all SHM models in that for $\gamma_q = 1$ we find the value $T = 170 \pm 10$ MeV, and for $\gamma_q \to 1.63$ a value $T \to 140$ MeV.

Test of SHM models—We have seen that hadronization of Ξ and ϕ is consistent with the three different SHM models, but there is an interesting constraint between T, γ_q arising from the constancy of the relative Ξ and ϕ yield. We see also in Fig. 2 that the variation of Ξ/K is significant, it changes by a factor of 2.3 in the entire data range. Considering that we already established by the study of Ξ/ϕ that the hadronization temperature does not vary, this indicates that there is a variation of the γ_s value by a factor of about 2.3 in the data range. We conclude that a fixed value $\gamma_s = 1$ cannot be chosen. This rules out the SHM model (a). We also note that this argument can be made in the same way considering the variation of the other ratios in Fig. 2 (e.g., Ξ/π and ϕ/K).

SHM results for Ξ/K and Ω/ϕ in the T, γ_s plane are shown in Fig. 4, obtained by the same method as before (i.e., using SHARE with other SHM parameters fixed at an appropriate value. For a given Ξ/K and/or Ω/ϕ a slight γ_q dependence remains since there are unrelated resonances decaying into K (and to a lesser degree Ξ). Thus we present for each fixed value of Ξ/K two extremes $\gamma_q = 1$ and $\gamma_q = \gamma_q^{\rm crit}$. The effect

TABLE II. Values of ratios Ξ/ϕ Eq. (1), Ξ/K Eq. (3), and Ξ/π and ϕ/π Eq. (4) obtained from the data and the resulting estimated uncertainty in γ_s and γ_q, respectively. When symbol "E" is shown in the error column, the data ratio is a result of the interpolation and/or extrapolation needed to account for different centrality bins.

Experiment	Centrality	$\Xi/\phi \times 10$	$\delta\gamma_q$	$\Xi/\mathrm{K} \times 10^2$	$\delta\gamma_s$	$\Xi/\pi \times 10^3$	$\phi/\mathrm{K} \times 10$	$\phi/\pi \times 10^2$
STAR 62	0–5%	3.04	E	4.19	9.6%	6.22	1.38	2.04
STAR 62	5–10%	3.00	E	4.08	9.2%	6.20	1.36	2.06
STAR 62	10–20%	2.94	E	4.06	9.3%	5.98	1.38	2.04
STAR 62	20–40%	2.88	12.5%	3.79	E	5.48	1.32	1.91
STAR 62	40–60%	2.85	14.6%	3.38	E	4.65	1.18	1.63
STAR 62	60–80%	2.49	19.3%	2.84	E	3.45	1.14	1.38
STAR 200	0–20%	3.02	11.8%	4.06	12.9%	6.04	1.34	$2.54^{+0.21}_{-0.09}$ [a]
SPS 80 AGeV	7%	3.33	24.5%	3.04	22.7%	2.60	0.83	0.88
SPS 40 AGeV	7%	2.45	42.1%	1.89	18.0%	3.23	0.78	0.83
SPS 30 AGeV	7%	2.57	66.5%	1.85	24.3%	2.10	0.63	0.72

[a]For STAR 200 ϕ/π considering Fig. 14 in Ref. [2] we give an average of data for centralities up to 50%.

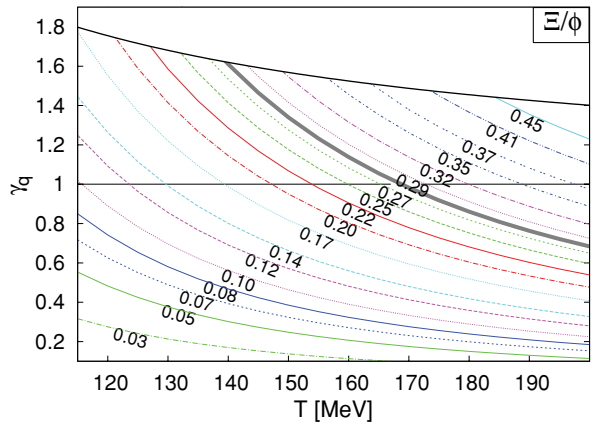

FIG. 3. (Color online) Lines of a constant given ratio Eq. (1) $\Xi/\phi \in [0.03, 0.45]$ in the T, γ_q plane. The lines for $\gamma_q = 1$ and $\gamma_q = \gamma_q^{\rm crit}$ are presented by solid black lines. The average result, 0.281, of all SPS and RHIC experiments is highlighted by a thick gray line. As this ratio is considered constant, this line indicates the prediction of the LHC results.

is depicted in Fig. 4(a) in terms of two lines shown by the same line type.

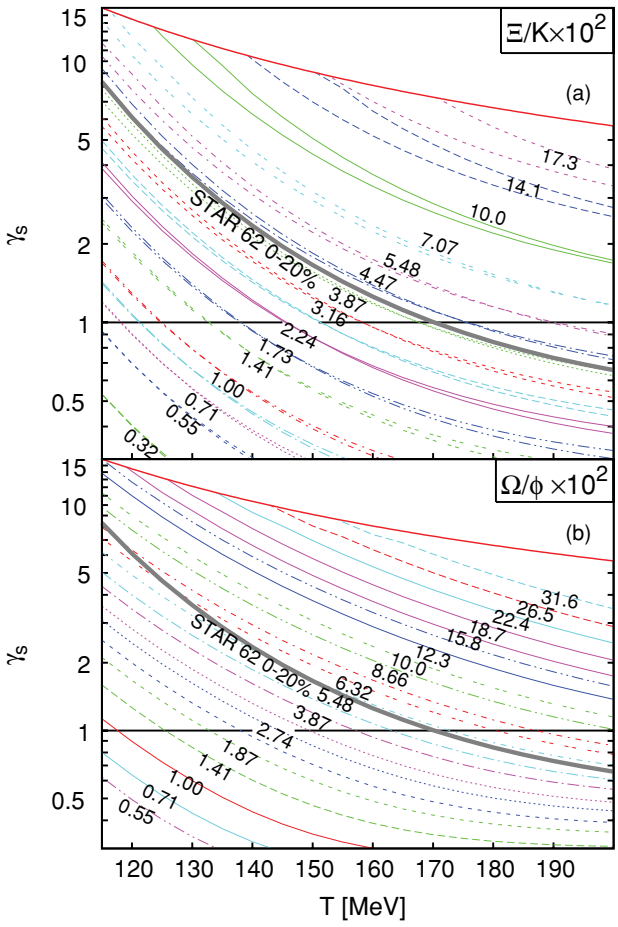

FIG. 4. (Color online) Lines of constant ratio Ξ/K (a) and Ω/ϕ (b). Experimental data from most central 0–20% STAR 62 are indicated by a thick line which in the bottom frame (b) shows our prediction. See text for more detail.

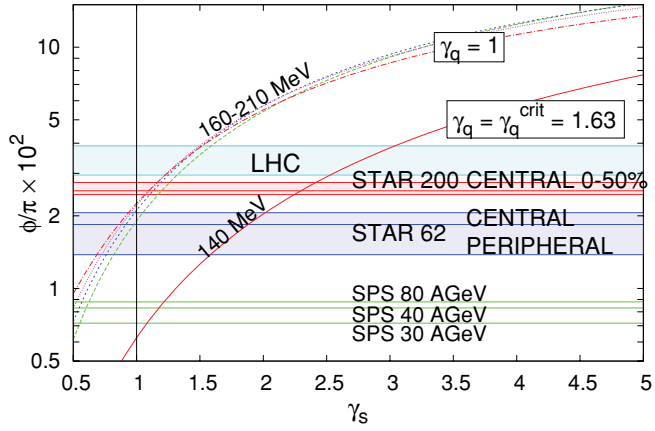

FIG. 5. (Color online) The relative ϕ/π Eq. (4) yield as a function of γ_s in several hadronization scenarios, see text. The vertical solid black line shows the chemical equilibrium with $\gamma_s = 1$. For experimental data see Table II. Predicted values for LHC are indicated in blue.

Note that similarly as for γ_q, there is a critical value for γ_s based on the Bose-Einstein condensation of the η meson ($\eta = 0.55(u\bar{u} + d\bar{d}) + 0.45 s\bar{s}$ [31,32]). The large values of γ_s can be relevant to the future LHC results. To compare theory and experiment we show the thick 0–20% STAR 62 line and by looking at the bottom frame of Fig. 4 we obtain the prediction $5.5 \times 10^{-2} < \Omega/\phi < 7.0 \times 10^{-2}$, the variation due to the variability of hadronization temperature.

To further elaborate the validity of models (b) and (c) we show on the right in Table II the ratios Ξ/π, ϕ/K and ϕ/π, where

$$\frac{\Xi}{\pi} \equiv \sqrt{\frac{\Xi^-\bar{\Xi}^+}{\pi^-\pi^+}}; \quad \frac{\phi}{K} \equiv \sqrt{\frac{\phi\phi}{K^-K^+}}; \quad \frac{\phi}{\pi} \equiv \sqrt{\frac{\phi\phi}{\pi^-\pi^+}}. \qquad (4)$$

The experimental Ξ/π and ϕ/π relative yields vary by a factor $\simeq$3.5 in both cases. In Fig. 5 we show the ϕ/π ratio and compare it to theory as a function of γ_s at a fixed given T. Model (b) with $T \simeq 140$, $\gamma_q = \gamma_{\rm crit}$ implies that the different experimental results correspond to $1 < \gamma_s < 2.4$. These values are consistent with the large value of $\gamma_q = \gamma_{\rm crit} \simeq 1.6$. However, for $\gamma_q = 1$, several fixed T lines nearly coincide in the interesting range $210 \geqslant T \geqslant 160$ MeV. This means that the growth in the yield of ϕ is nearly compensated by the growth in the π multiplicity. It will be very interesting to see how LHC results will line up in this presentation since we see that the high-energy RHIC results even at $\gamma_q = 1$ imply $\gamma_s > 1$. A value $\gamma_s > 1$ is incompatible with the picture of strangeness production in hadron collisions and implies the presence of a strangeness dense QGP phase as a source of hadrons.

Behavior at LHC—As already remarked the ratio $\Xi/\phi \simeq 0.28$ is firmly constrained and cannot change. Even under the extreme LHC conditions we expect that this ratio will be the same as at RHIC. However, considerable changes can be expected for the other (multi)strange particle ratios that were discussed earlier [33,34]. Here we will mainly address the ϕ/π ratio.

When we accept the premise that entropy and strangeness are conserved during the hadronization, we can predict values of the phase-space occupancy γ_s in chemical semiequilibrium and nonequilibrium models for the LHC. We expect a 20% increased value of strangeness over entropy $s/S \simeq 0.037$ [34]. For the two models under consideration ($T = 140$ MeV,$\gamma_q = \gamma_q^{\text{critical}}$ and 170 MeV,$\gamma_q = 1$) this value suggests [33] $\gamma_s/\gamma_q \simeq 1.55$. The expected ϕ/π ratio is 2.95×10^{-2} and 3.90×10^{-2} for the two models as indicated by the boundaries of the LHC band in Fig. 5. Experimental results of this magnitude require $\gamma_s > 1$ and concludes in favor of chemical nonequilibrium, the still ongoing discussion of chemical equilibrium models.

Summary and conclusion—We find that the relative particle yield Ξ/ϕ is practically constant as a function of centrality and the reaction energy at RHIC and SPS. We find that these particles, despite their small reaction cross-sections are emerging at the same hadronization condition as all bulk particles. This result was anticipated [35] for a fast expanding QGP fireball, which undercools and rapidly breaks apart (hadronizes) and was used extensively in single hadronization models [16,18,19,22].

Variation in the ratio Ξ/K (and thus also $\phi/K \propto \gamma_s/\gamma_q$) implies a variation in strange phase-space occupancy γ_s, in agreement with the expectation that strangeness production grows with energy and the centrality of the collision. This experimental result is incompatible with the chemical equilibrium model (a), for which also the parameter γ_s is fixed to 1 by definition.

Considering further the yields Ξ/π and ϕ/π, consistency with the bulk matter particle production rates is arrived at within the chemical nonequilibrium model (b) with $\gamma_q > 1$ and $\gamma_s > 1$. These values imply that the observed strange hadrons yields are above chemical equilibrium, a feature predicted to be signature for hadronization of a QGP fireball [36]. The expected further increase of $\gamma_s > 1$ at LHC implies a further increase of the ϕ/π ratio, providing a clear distinction between chemical nonequilibrium model (b) and semi-equilibrium model (c).

Our results show that the yields of all multistrange hadrons available today are (1) compatible with the SHM picture of hadron formation, (2) are well described by current chemical nonequilibrium hadronization models in the parameter domain obtained from the other hadron yields, and (3) these data are incompatible with the chemical equilibrium single-freeze-out SHM. A critical test of our approach is that in LHC ion experiments the Ξ/ϕ ratio remains the same as was observed at SPS and RHIC.

Acknowledgments—JR would like to thank Z.L. Matthews and O. Villalobos Baillie of Birmingham University and CERN-ALICE collaboration for interesting discussions. This work was supported by a grant from the US Department of Energy, DE-FG02-04ER41318.

[1] A. R. Timmins (STAR Collaboration), Nucl. Phys. A **830**, 829c (2009).
[2] B. I. Abelev (STAR Collaboration), Phys. Lett. B **673**, 183 (2009).
[3] C. Alt (NA49 Collaboration), Phys. Rev. C **78**, 044907 (2008).
[4] C. Alt (NA49 Collaboration), Phys. Rev. C **78**, 034918 (2008).
[5] J. Adams (STAR Collaboration), Phys. Rev. Lett. **98**, 062301 (2007).
[6] J. Speltz, Ph.D. thesis, Institut Pluridisciplinaire Hubert Curien, Strasbourg, France, 2006.
[7] B. I. Abelev (STAR Collaboration), Phys. Rev. C **79**, 034909 (2009).
[8] I. Kuznetsova, J. Letessier, and J. Rafelski, Acta Phys. Pol. B **40**, 1013 (2009).
[9] Z. L. Matthews (ALICE Collaboration), J. Phys. G: Nucl. Part. Phys. **37**, 094048 (2010).
[10] J. Letessier and J. Rafelski, Camb. Monogr. Part. Phys. Nucl. Phys. Cosmol. **18**, 1 (2002).
[11] G. Torrieri *et al.*, Comput. Phys. Commun. **167**, 229 (2005); **175**, 635 (2006).
[12] F. Becattini and R. Fries (2009), arXiv:0907.1031.
[13] Z. Fodor and S. D. Katz (2009), arXiv:0908.3341.
[14] P. Braun-Munzinger and J. Wambach, Rev. Mod. Phys. **81**, 1031 (2009).
[15] G. Torrieri and J. Rafelski, New J. Phys. **3**, 12 (2001).
[16] J. Rafelski, J. Letessier, and G. Torrieri, Phys. Rev. C **72**, 024905 (2005).
[17] J. Letessier and J. Rafelski, Phys. Rev. C **73**, 014902 (2006).
[18] J. Letessier and J. Rafelski, Eur. Phys. J. A **35**, 221 (2008).
[19] J. Rafelski and J. Letessier, J. Phys. G **36**, 064017 (2009).
[20] R. Gupta (2009), arXiv:0912.1374.
[21] F. Becattini, J. Cleymans, A. Keranen, E. Suhonen, and K. Redlich, Phys. Rev. C **64**, 024901 (2001).
[22] W. Broniowski and W. Florkowski, Phys. Rev. C **65**, 064905 (2002).
[23] F. Becattini, M. Gazdzicki, A. Keranen, J. Manninen, and R. Stock, Phys. Rev. C **69**, 024905 (2004).
[24] F. Becattini, J. Manninen, and M. Gazdzicki, Phys. Rev. C **73**, 044905 (2006).
[25] F. Becattini and J. Manninen, J. Phys. G **35**, 104013 (2008).
[26] R. Hagedorn and J. Ranft, Nuovo Cimento Suppl. **6**, 169 (1968).
[27] R. Hagedorn and J. Rafelski, Phys. Lett. B **97**, 136 (1980).
[28] J. Rafelski and J. Letessier, Nucl. Phys. A **715**, 98 (2003).
[29] C. Alt *et al.* (NA49 Collaboration), Phys. Rev. C **77**, 024903 (2008).
[30] S. V. Afanasiev (NA49 Collaboration), Phys. Rev. C **66**, 054902 (2002).
[31] V. Uvarov, Phys. Lett. B **511**, 136 (2001).
[32] J.-W. Li and D.-S. Du, Phys. Rev. D **78**, 074030 (2008).
[33] I. Kuznetsova and J. Rafelski, Eur. Phys. J. C **51**, 113 (2007).
[34] J. Letessier and J. Rafelski, Phys. Rev. C **75**, 014905 (2007).
[35] J. Rafelski and J. Letessier, Phys. Rev. Lett. **85**, 4695 (2000).
[36] M. Jacob and J. Tran Thanh Van, Phys. Rep. **88**, 321 (1982), see p. 331 ff.